scientific reports

Check for updates

OPEN

Prediction of water level at Huayuankou station based on rating curve

Ming Li[1], Zhao Zheng[2,3], Chaojie Niu[1]✉, Liyu Quan[1], Chengshuai Liu[1], Xiang Li[1], Chen Shi[1], Dongyang Li[2], Lianjun Zhao[4], Shasha Han[4,5] & Caihong Hu[1]✉

The construction of large reservoirs has modified the process of water and sediment transport downstream, resulting in changes in the morphology of the river cross-section. Changes in water and sand transport and cross-sectional morphology are reflected in the rating curve at the cross-section. This study analyzed the variations in the rating curve at the Huayuankou (HYK) section and their influencing factors, and conducted water level predictions based on this relationship. The findings revealed that while the annual mean water level has shown a declining tendency over the past 20 years, the annual mean discharge has shown a constant pattern. The rating curve at this stretch narrowed from a rope-loop type curve in its natural condition to a more stable single curve as a result of the construction of the dam upstream of the HYK section. The effect of pre-flood section morphology and the water–sediment process on the scattering degree of the rating curve is inverse; increasing roughness and hydraulic radius decreases scattering degree, while increasing sand content and sand transport rate increases scattering degree. Using the measured data from 2020 as an example, the feasibility of predicting cross-sectional water levels using the rating curve was verified. The prediction results were accurate when the flow was between 1000 and 2800 m^3/s; However, when the flow was between 2800 and 4000 m^3/s, the forecast results were typically slightly lower than the measured values. Overall, the method demonstrates good predictive accuracy. Insight from the method can be used to predict water levels to better inform decision making about water resources management, and flood emergency response in the lower Yellow River.

Keywords Rating curve, Huayuankou, Cross-sectional morphology, Water level prediction

The purpose of constructing a large number of reservoirs around the world is to control river floods, store water for irrigation, and generate hydroelectric power. However, this inevitably has an impact on the hydrological processes of river ecosystems[1]. The construction and operation of reservoirs in river basins have a significant impact on river flow, sediment transport, channel morphology, and riverine ecosystems[2–7]. Some scholars, after evaluating the impact of dam construction on downstream water conditions, have pointed out that the duration and magnitude of river flow and peak flow change after the construction of dams[8–14]. After the construction of the Garrison Dam on the upper Missouri River in the United States, the peak flow decreased from an extreme value of 10,279 m^3/s upstream of the dam to 4390 m^3/s[12]. In the Mekong River, reservoirs cause an increase in average monthly flow by 25–160% during the non-flood season (December–May) and a decrease by 3–53% during the flood season (June–October)[13]. Some studies[14–18] evaluating the impact of dam construction on hydrological conditions and sediment transport have found that the construction of dams has led to significant changes in sediment flux in many of the world's major rivers, such as the Mississippi River[19] in the United States, the Nile River[20] in Egypt, the Yangtze River[21,22], and the Yellow River[23–25] in China. Sediment trapping by dams in the global hydrologic north has contributed to global sediment flux declines to 49% of pre-dam conditions[26]. In addition, in the early twenty-first century, approximately 25–30% of the sediment flux in coastal environments was intercepted by existing dams[27,28]. Dams and reservoirs have greatly altered the water discharge and sediment conditions in their downstream rivers.

[1]School of Water Conservancy and Transportation, Zhengzhou University, Zhengzhou 450001, China. [2]Henan Yellow River Engineering and Consulting Co., LTD, Zhengzhou 450003, China. [3]Henan Engineering Research Center for Protection and Governance of Yellow River, Zhengzhou 450003, China. [4]Yellow River Institute of Hydraulic Research, YRCC, Zhengzhou 450003, China. [5]State Key Laboratory of Hydro-science and Engineering, Tsinghua University, Beijing 100084, China. ✉email: 202021221010285@gs.zzu.edu.cn; hucaihong@zzu.edu.cn

To adapt to the changes in water and sediment caused by dam construction, downstream river sections may experience phenomena such as riverbank erosion and water level adjustments[29–31]. The stability of river ecosystems, production and domestic water consumption in coastal areas, the ecological environment, and the safety of flood control are all directly impacted by changes in water level[32]. Due to the river channel's low water level, it is challenging to support life and economic activity near the coast; on the other hand, a high water level will inundate the floodplain and raise the risk of flooding[33].The change of water level is affected by many factors, such as the scouring and sedimentation of the river bed, the constriction of the river channel, the change in roughness, and the backwater caused by the dense vegetation. These are all important factors in the change of water level. However, aside from vegetation, dam development is generally to blame for the changes in the aforementioned variables. After the construction of the Aswan Dam on the Nile River in Egypt[34], the lower river channel was cut down by an average of 0.45 m, and the water level of the same flow showed a downward trend. Similarly, the Tagliamento, Piave and Brenta rivers in Italy were cut down 4–6 m after the dam was put into use[35]. Although the flood flow of the Mississippi River in the United States in 2011 was lower than it was in 1927 and 1973, the flood level rose as a result of backwater brought on by dense vegetation in the floodplain's upper reaches[36]. After the construction of a reservoir in the Missouri River in the United States, the low water level fell by more than 2.5 m[37], while the downstream flood level around Kansas City rose by nearly 1 m. In China, the Danjiangkou Dam on the Han River and the Three Gorges Dam on the Yangtze River[33,38–40] both lowered the water level at the same river discharge at the downstream hydrological stations. However, after the completion of the dam, the changes in water levels across different rivers were not uniform[33]. The middle sections of the Yangtze River's high water level have decreased since the Three Gorges Dam began operating, however the flood water level under the same flow has not showed a declining trend[41] and some studies even indicate that the water level has increased[42]. In short, affected by many factors, the change of water level itself is an extremely complex hydrological process.

The hydraulic law indicates that under appropriate conditions, there exists a unique and stable relationship between water level and discharge, which can be described using a rating curve[43]. However, due to complex variations in water levels, there is significant uncertainty in the rating curve[44]. Due to the difficulty in measuring discharge accurately, scholars often use rating curves for discharge prediction[43,45–47]. This curve only requires water level data to indirectly estimate discharge[48]. Some scholars also use rating curves for tasks such as water depth parameter calibration[49], calculating annual peak water levels[50], and predicting tidal river water levels[51]. The Yellow River was once the river with the highest sediment load in the world. However, since the construction and operation of the Xiaolangdi Reservoir, the sediment concentration in the water has significantly decreased due to the interception of sediment by the reservoir[52]. Furthermore, the Lower Yellow River has transitioned from short-duration high-discharge conditions to long-duration moderate-low discharge conditions. Under the long-term influence of low-sediment water, the downstream river channel has shifted from a state of continuous sedimentation to a state of continuous erosion[53]. This change has led to great uncertainty in the water level-discharge relationship in the lower reaches of the Yellow River. Currently, scholars have made significant progress in the study of the lower reaches of the Yellow River[54–58]. However, most of the research has focused on land use changes in the lower Yellow River[59,60], variations in sediment element content and heavy metal concentrations in the water[61,62], and the coordinated development of multiple systems such as the economic environment[63]. Yet, the lower Yellow River, being a flood-prone area[64–66], remains under-researched. Few scholars have investigated and predicted the water level-discharge relationship in the lower reaches of the Yellow River. Therefore, studying the rating curve of key hydrological stations in the lower Yellow River is of great practical significance for flood control in the floodplain. This study proposes a water level prediction method for the HYK statio's rating curve, which can accurately predict the water level-discharge relationship. This method enables early flood warning during the flood season, thereby ensuring the safety of the lives and property of downstream residents. Insight from the study can be used to predict water levels to better inform decision making about water resources management, and flood emergency response in the lower Yellow River. This study focuses on the variation patterns and influencing factors of the water level-discharge relationship at the HYK hydrological station in the lower Yellow River. The objectives are: A) to use Ensemble Empirical Mode Decomposition (EEMD) to decompose the annual average water level and annual average discharge at the HYK hydrological station, analyze the trends in water level and discharge; B) analyze the corresponding relationship between water level and discharge during different periods, study the impact of different reservoir operations on the rating curve in the lower Yellow River; C) study the influencing factors of changes in the rating curve, and establish a water level prediction method based on the rating curve.

Study area

The Yellow River has a length of 5464 km and a basin size of 752,000 km^2. Lower Yellow River reaches, with a river length of 786 km and a downstream area of 23,000 km^2, are located below Taohuayu. According to the natural form of the river and the change of river potential, the lower reaches of the Yellow River can be divided into wandering river section (Tiexie–Gaocun), transitional river section (Gaocun–Taochengpu) and curved river section (Taochengpu–Lijin), with the estuary section below Lijin. The division of the Yellow River is shown in Fig. 1a. The hydrological station in the initial downstream reach is the HYK hydrological station. Figure 1b shows the riverbed elevation at different distances within 10,000 m downstream from the HYK cross-section as the starting point, as measured data.

The HYK hydrographic station is a crucial control and observation point along the Yellow River's lower reaches. A total of 730,000 km^2—roughly 97 percent of the Yellow River basin—makes up its control basin. Strong oscillations in this section's main channel make the morphology and water–sand conditions very sensitive to changes in the water and sand entering the system from upstream. For the purpose of examining the development of the lower Yellow River channel, HYK Station's examination of water and sand variation serves

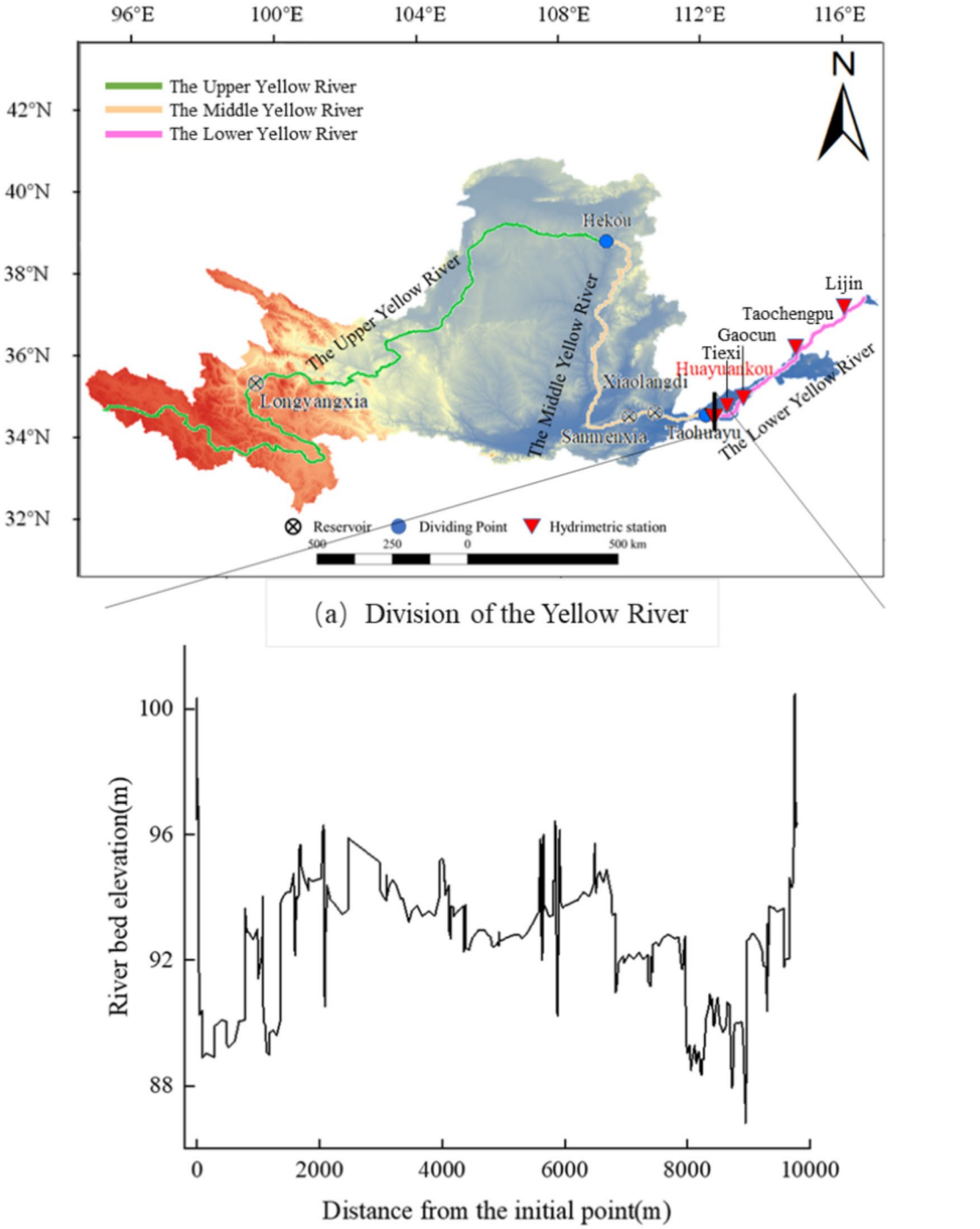

Fig. 1. Overview of the study area.

as both a prerequisite and a starting point. Additionally, the analysis of the rating curve at this section can aid in flood prediction and early warning for the downstream section of the river as well as the upstream reservoir to transfer water and sand. The water potential of this station also partially reflects the actual situation of water and sand entering the downstream.

Daily average water level and daily average river discharge at the HYK section from 1949 to 2020 were obtained from the Yellow River Conservancy Commission. The measured river discharge of flood events from 2006 to 2020 and their corresponding water levels were obtained from the Yellow River Hydrological Yearbook (2006–2020), the data are considered accurate and reliable.

Method and material

Ensemble empirical mode decomposition (EEMD)

For the multi-timescale analysis of time series, Huang[67] proposed Empirical Mode Decomposition (EMD) that can separate the fluctuations of different timescales step by step, namely the Intrinsic Mode Function (IMF). This is a new method for handling nonlinear and non-stationary data series. It can linearize and smooth the data, preserving their characteristics during decomposition. The result includes trend components and fluctuation components of various scales, with the fluctuation components defined as IMF across different time scales. Each IMF needs to satisfy the following two conditions: (1) The number of extreme values in the whole signal data sequence must be equal to the number of over zeroes or differ by at most one; (2) At any moment, the average value of the envelope of local maxima (upper envelope) and the envelope of local minima (lower envelope) must be zero. Model mixing means that a single IMF mixes different frequency components, or different IMFs contain the same frequency components, and is a major drawback of empirical model decomposition that is difficult to avoid. To solve this problem, white noise is added to the signal to be decomposed, facilitating the separation of the different scales of the input data[68,69]. The decomposition steps of EEMD are as follows:

(1) The original signal data sequence $x_i(t)$ is supplemented with Gaussian white noise $w_i(t)$ to obtain the signal to be processed after noise addition. The new sequence can be calculated as Eq. (1).

$$x_i(t) = x(t)+w_i(t) \tag{1}$$

(2) Decomposition of the new data sequence into IMFs using the method of EMD to decompose the signal to be processed.
(3) Repeat the above steps with different white noises.
(4) Calculate the average of the corresponding IMFs obtained at each stage as the final result. Refer to Eq. (2) for the calculation.

$$c_j=\frac{1}{N}\sum_{i=1}^{N} c_{j,I} \tag{2}$$

where N is the ensemble times of adding noise, c_j reparents the j-th IMF component; $c_{j,I}$ is the i-th IMF when adding the ith noise.

Methods for variance assessment

Ma Bingyan suggested three techniques to determine the variance of various indicators, including the angle method, the area method, and the distance method, in order to assess the sensitivity of the parameters in the Storm Water Management Model (SWMM)[70]. Due to the influence of rating curve, this study adopts the area method for calculating the variance. Equation (3) is the area method, using curves c_a and c_b to fit rating curve. Then using area (A) enclosed by the two curves c_a and c_b represent the difference between the scattered sequences. The larger A is, the greater difference between the two curves. S for degree of variation, the larger S represents a greater degree of variation.

$$S = \frac{A}{Q_0 - Q_1} = \frac{\int_{Q_0}^{Q_1} (C_a - C_b)dQ}{Q_0 - Q_1} \tag{3}$$

where S, represent degree of variation by the area methods; A represents the area of the inner envelope between the two curves; Q_0 and Q_1 are the minimum and maximum discharge of floods in different fields.

Water level forecast method

This study uses the rating curve to predict the water level. Depending on specific factors, such as whether the rating curve is a single value function, the rating curve can be classified as either stable or unstable. The function was fitted by correlation analysis in order to objectively represent the rating curve, and the degree of variation (S) was proposed to highlight the stability of the rating curve following analysis. First, based on the cross-sectional data, water level data, and river discharge data from the HYK station, the width-depth ratio (B), water surface slope (J), dispersion (W), and roughness (n) were calculated. The linear change in the relationship between the daily average water level and discharge at different stages for the HYK section was analyzed to determine the critical value of W under the 95% prediction band, was determined to be 21. If the W value is below 21, it indicates that the water level-discharge relationship points are stable, making the area method suitable for prediction. Conversely, if the W value exceeds 21, the relationship points are scattered, rendering the area method unsuitable for prediction. When W meets the criteria, the area method can be used to determine the envelope range (A) and the variation (S) of the curve. The relationships between B, J, and S are compared, and value of S for different magnitudes for the predicted year is assessed. The water level prediction equation's parameters (see Eq. 4) are determined through linear regression analysis. Finally, the relationship between the forecasted year water levels and river flows is examined. The prediction technical route is shown in Fig. 2.

$$Z = a * \ln(Q) + b \tag{4}$$

In which, Q represents discharge, and Z represents the water level corresponding to that discharge, a, b are parameters.

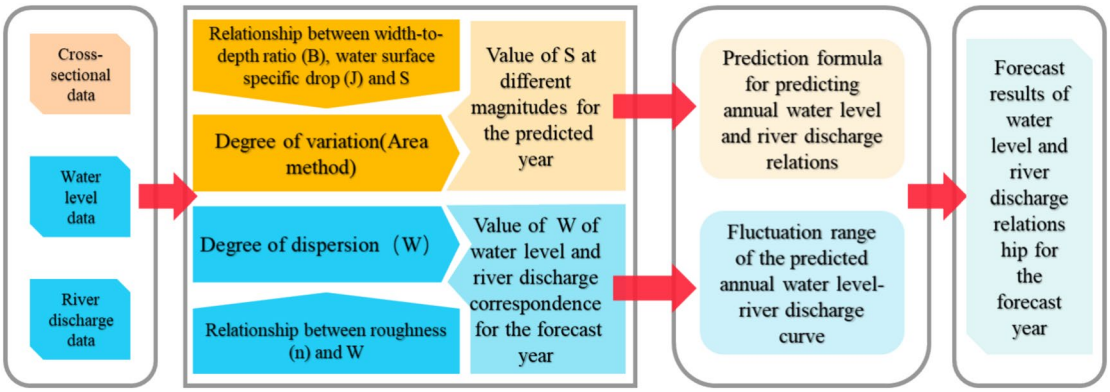

Fig. 2. Water level prediction technology roadmap.

Results

EEMD decomposition of water level and river discharge

Five eigenmodal functions (c_1–c_5 components) and one residual trend term (Res component) were obtained from the EEMD decomposition of a total of 72-years time series of annual mean discharge and annual mean water level from 1949 to 2020 at the HYK section. By using empirical mode decomposition and residual trend terms, periodic variations and trends in mean annual flow and mean annual water level can be obtained. These results are depicted in Fig. 3.

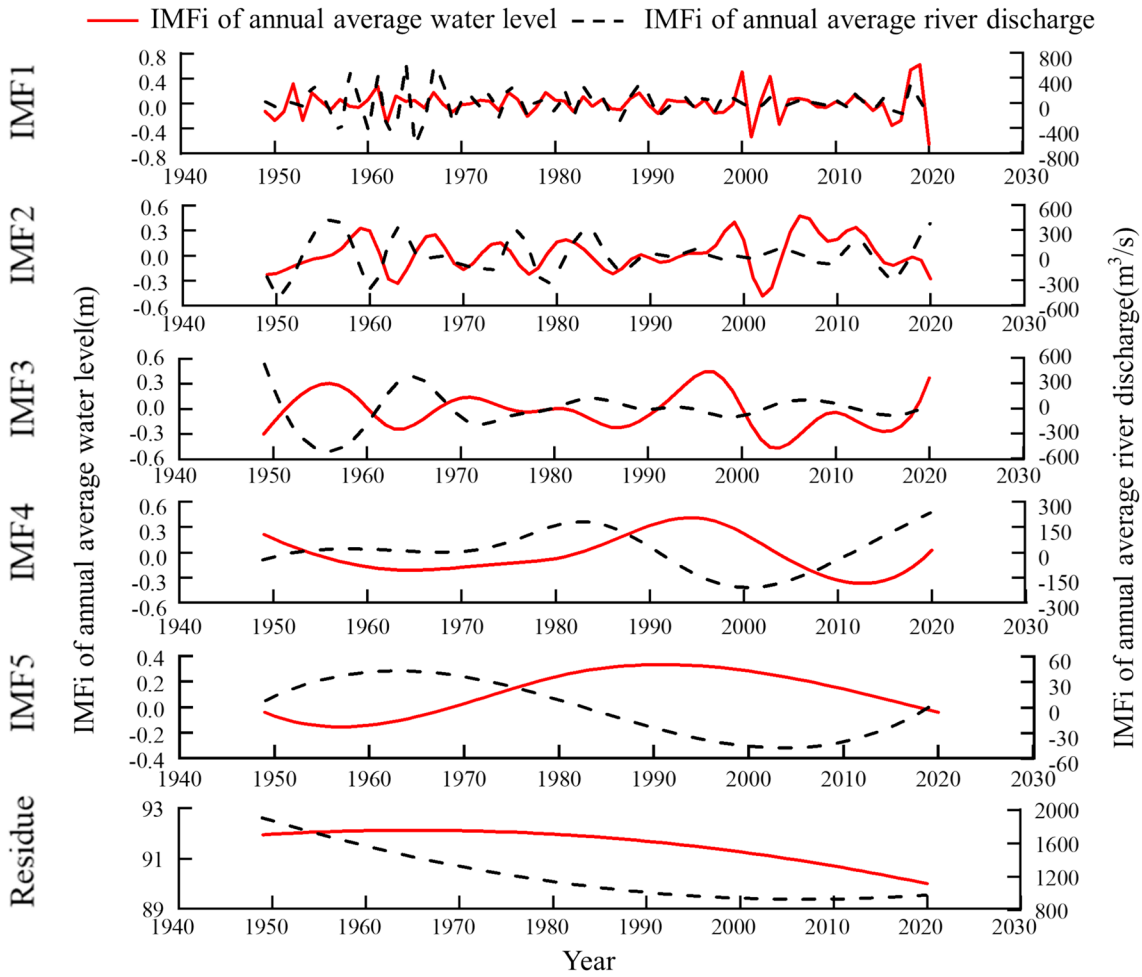

Fig. 3. Annual average discharge and annual average water level through EEMD decomposition.

(1) The process of annual average discharge and water level in the HYK section is non-linear and non-stationary, as can be observed from the above figure. The time series' annual mean discharge and annual mean water level are both the results of the combined action of several fluctuation components. These components can be divided into five oscillatory components with various fluctuation periods and one trend component, which reflects the multi-timescale characteristics of the annual mean water level and flow variation at the HYK section.
(2) The quasi-periods corresponding to the c_1 component of the annual mean discharge and the annual mean water level are about 3.13a and 3.27a, the quasi-periods of both the c_2 component are 8a, the quasi-periods of both the c_3 component are 14.4a, the quasi-periods of the c_4 component are about 40a and 42.35a, and the quasi-periods of the c_5 component are about 65.45a and 60a.
(3) The Res component displays the general trend for both the average annual river discharge and water level. The annual average discharge of the HYK section significantly decreased from 1949 to 2000 as a result of the construction of the major reservoirs; after 2000, however, as a result of the operation of the Xiaolangdi reservoir, the discharge of the HYK section was directly impacted by the discharge of Xiaolangdi and essentially stabilized. The average yearly water level was essentially steady from the 1940s until the 1980s. Due to the management of the Yellow River by the management agencies, the lower Yellow River's siltation improved after the 1980s and the average annual water level declined quickly.

Influence of reservoirs construction on the rating curve

On the Yellow River's main course, three reservoirs have been constructed since New China's foundation. In chronological order, they are Sanmenxia Reservoir (SMXR), Longyangxia Reservoir (LYXR), and Xiaolangdi Reservoir (XLDR). The research period (1950–2020) was divided into four stages based on the time when the reservoir was put into use, namely the natural state (1950–1959), the operation stage of SMXR (1960–1985), and the operation stage of LYXR (1986–1999) and the operation stage of XLDR (2000–2020).

In this study, two representative years from various reservoir operation stages were selected to analysis the relationship between the daily average water level (Z) and discharge in order to reflect the change in the rating curve at the HYK section (Fig. 4). The rating curve is a typical rope type in its natural form (1957 and 1958), and the highest daily average flow in the chosen years is greater than 10,000 m^3/s. The rope-shaped curve in the natural state has transformed to a comparatively dispersed single curve after the operation of the SMXR (1979 and 1984). The linear shape has been greatly constrained. Additionally, the maximum daily average flow has fallen by more than 50% as a result of human activity. Although LYXR is a large-scale reservoir on the Yellow River, it can regulate the water and sediment conditions in the downstream reaches of the reservoir, but because it is located in the upper reaches of Qinghai Province, it is more than 1500 km away from HYK Water Section, and there is SMXR between them. Therefore, the influence of LYXR on HYK Section (1989 and 1990) is weakened. From e (2006) and f (2016) of Fig. 4, compared with the previous stage, the rating curve of HYK section has not changed greatly. Xiaolangdi Dam is located 129.7 km upstream of HYK section. It is the closest of the three dams to this section, so it has the strongest constricting effect. It can be seen from the g and h in Fig. 4 that the rating curve of HYK section in 2006 and 2016 are stable single curves.

Classification of rating curve after the completion of Xiaolangdi Reservoir

The results of fitting the rating curve of several floods that occurred at the HYK station during the course of the previous 14 years are displayed in Fig. 5.

With the exception of a few years, the majority of in-year flood events follow a single curve and are generally stable. Considering the inconsistent changes in the occurrence of floods of different magnitudes, the flood discharge is divided into two grades of 1000–2000 and 2000–4000 m^3/s according to the size of flood flow in recent years (The flood events in 2016 and 2017 at the HYK section did not fall between 2000 and 4000 m^3/s, so they did not participate in the second level of calculation). Taking 2010, which is in the center of the line cluster, as the benchmark, the variance between the fitted function curves of different years and the fitted function curves of 2010 is calculated. The curves of different years are classified based on the variance. The calculation results are shown in Table 1.

Based on the calculation results in the table, it is easy to see that there has been a change in the rating curve in recent years, indicating a decrease in water level at the same flow rate. In addition to this the curves for higher flow rates are decreasing more sharply. Scatter plots were plotted for fitting (Fig. 6), and the fitted straight lines had a strong downward trend, and all single-value correlations reached a degree of 0.95 or higher.

Influencing factors of rating curve

In general, the rating curve is influenced by the section conditions (roughness, hydraulic radius, overflow area, etc.) and water and sand conditions (sand content, incoming sand coefficient, etc.). In order to predict the range of water level change under the same discharge by using the rating curve through the section condition and sand content of pre-flood, the influencing factors of rating curve are analyzed here from two perspectives of line and fitted curve.

Factors influencing the dispersion of the rating curve

The rating curve is used to reflect the correspondence between discharge and water level. During the course of the study, it was found discovered that the ratio of discharge to water level somewhat predicts the dispersion of the scattered points; more specifically, the larger the ratio of discharge to water level, the higher the dispersion, at which time the rating curve resembles the type of rope set. Therefore, W (ratio of discharge to water level) is

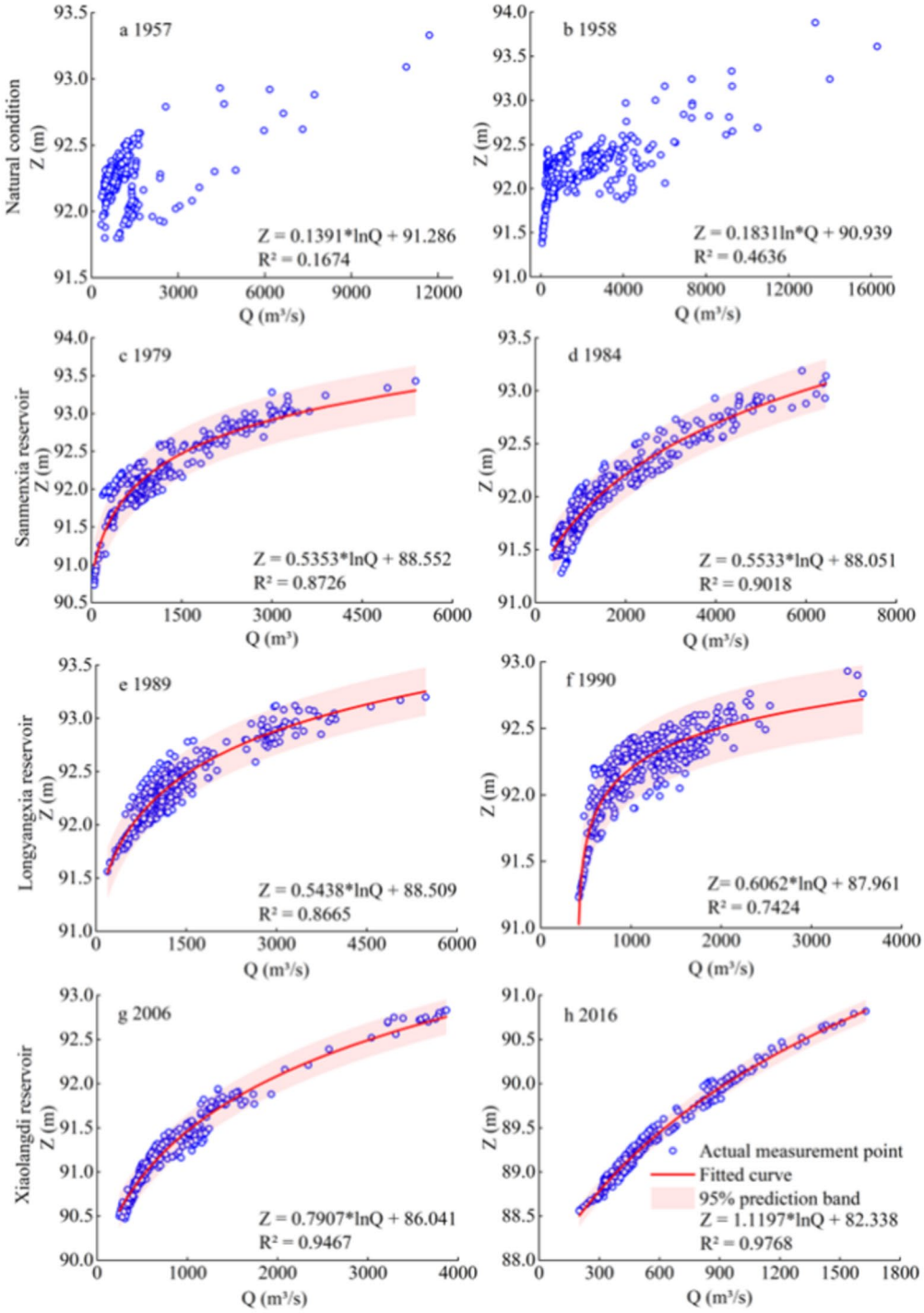

Fig. 4. The linear change of the relationship between the daily average water level and discharge of HYK section at different stages.

used as an index reflecting the degree of scattering dispersion to analyze its closely related section conditions as well as water and sand conditions.

Figure 7 shows the correspondence between *W* and pre-flood section conditions (roughness, overland flow area, hydraulic radius, and water surface slope). As shown in the figure, the cross-sectional overflow area and the water surface slope from the HYK cross-section to the Tiexi cross-section have no correlation with the rating curve at the HYK. Relatively speaking, both roughness and hydraulic radius have a large effect on *W*, and the value of *W* decreases with the increase of roughness and hydraulic radius. This means that the rating curve at the HYK section is more stable as the roughness and hydraulic radius increase.

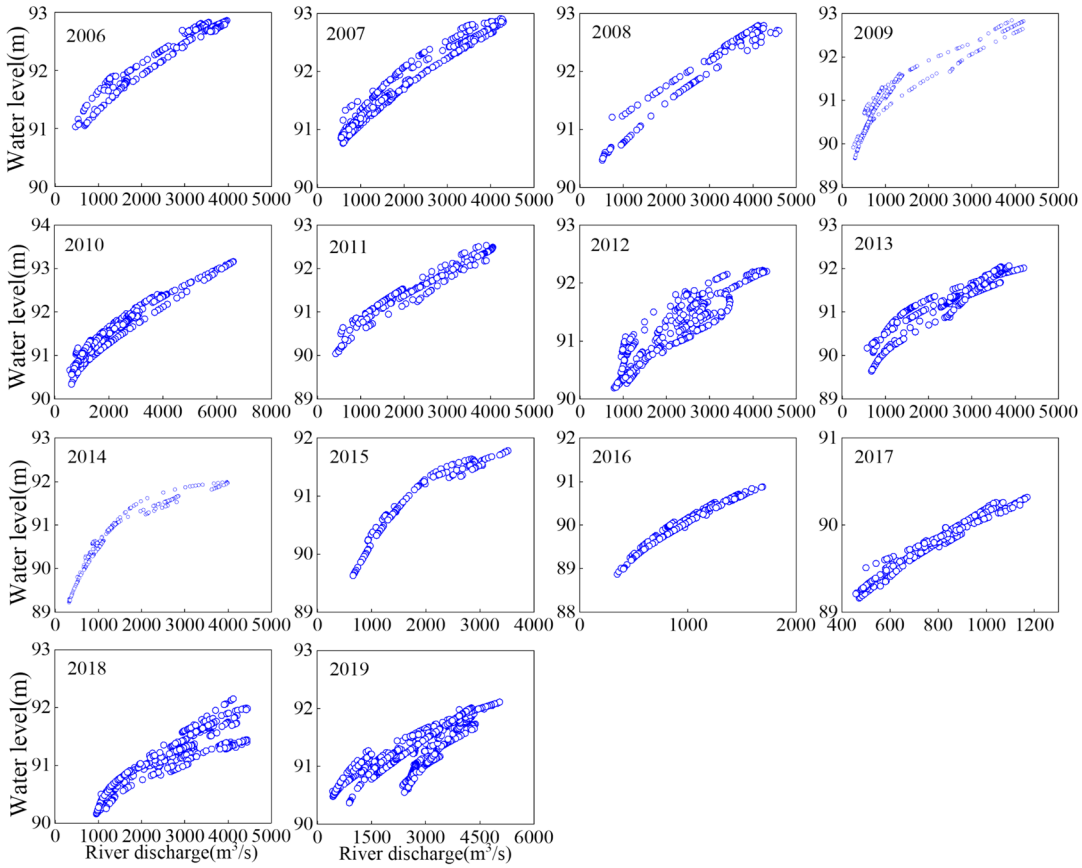

Fig. 5. Flood events in different years from 2006 to 2019.

	1000–2000 (m^3/s)	2000–4000 (m^3/s)
2006	503.8	1177.75
2007	227.19	618.41
2008	263.35	936.75
2009	269.24	631.09
2010	–	–
2011	66.61 (–)	78.61 (–)
2012	370.10 (–)	595.12 (–)
2013	487.37 (–)	807.15 (–)
2014	285.42 (–)	497.36 (–)
2015	524.53 (–)	705.55 (–)
2016	622.90 (–)	–
2017	771.48 (–)	–
2018	594.49 (–)	1338.93 (–)

Table 1. The variance between different years and the base year calculated by the area method. Area of + means the curve is above the base year, area of − means the curve is below the base year.

Figure 8 shows the correspondence between W and the water and sand conditions (sediment concentration (H) and sand transmission rate (T)) during the flood season. The figure shows that the scattering of water level-discharge points has a high degree of correlation with the sand content and transmission rate. When the sand content is higher than 5 kg/m^3, the tendency of dispersion increasing with the sand content decreases; the dispersion increases with the increase of sand transport rate.

Changes in cross-sectional conditions as well as water and sand conditions can cause changes in the degree of scattering of water level-discharge points. But these two types of factors have the opposite effect, the increase of roughness and hydraulic radius will lead to a more stable rating curve, while the increase of sand content and sand transport rate will lead to a more rope set type of rating curve.

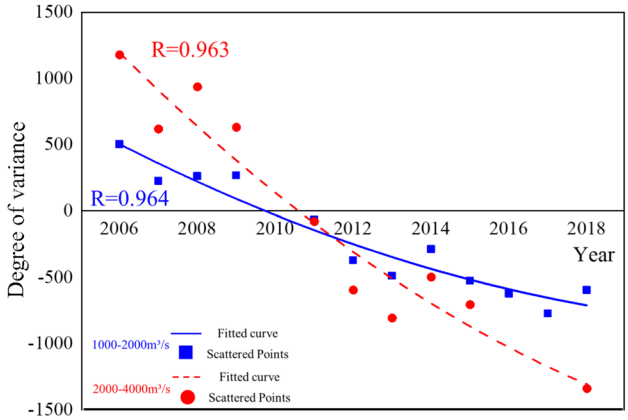

Fig. 6. Trends in the variance of fitted curves at different flood magnitudes.

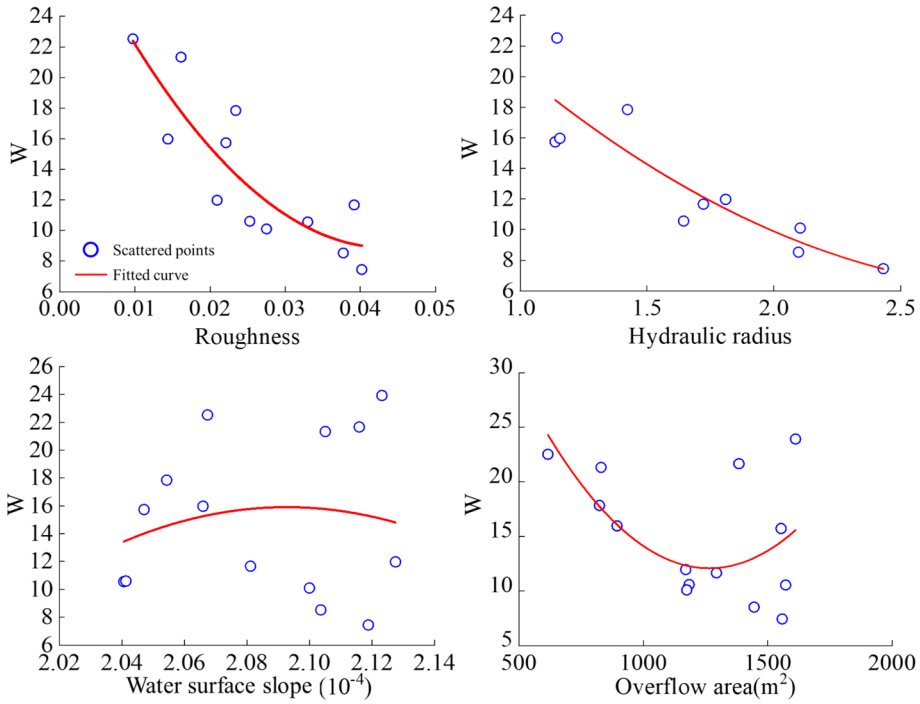

Fig. 7. The correspondence between W and pre-flood section conditions.

Factors influencing the variation between water level and discharge

As above, the area method was used to divide the lower discharge (1000–2000 m^3/s) and higher discharge (2000–4000 m^3/s) in the rating curve from 2006 to 2020 into two categories each. Here, the factors affecting the rating curve at lower discharge and higher discharge are analyzed in terms of section conditions and water and sand conditions respectively.

Figures 9 and 10 shows the degree of variation of the fitted curve of water level and discharge for each year from 2006 to 2020 at the HYK section for the lower discharge and the higher discharge and the degree of fitting between various factors for the lower discharge and higher flow rate. The figure shows that there is a high degree of correlation between both width-to-depth ratio and water surface slope and the degree of variance, while the influence factors in other section conditions and discharge conditions have a low effect on the degree of variance. As the aspect ratio decreases, the variance turns negative and the absolute value gradually increases. In contrast, the variance shifts to negative values and increases in absolute value as the water surface slope decreases. The R^2 values for the high flow in the width-depth ratio and water surface drop plots are 0.91 and 0.88, respectively. For the low flow, the R^2 values in the width-depth ratio and water surface drop plots are 0.89 and 0.93, respectively. Compared with the fitting degree of low flow, the fitting degree of the high flow and width-to-depth ratio is higher, and the fitting degree of water surface gradient is relatively lower.

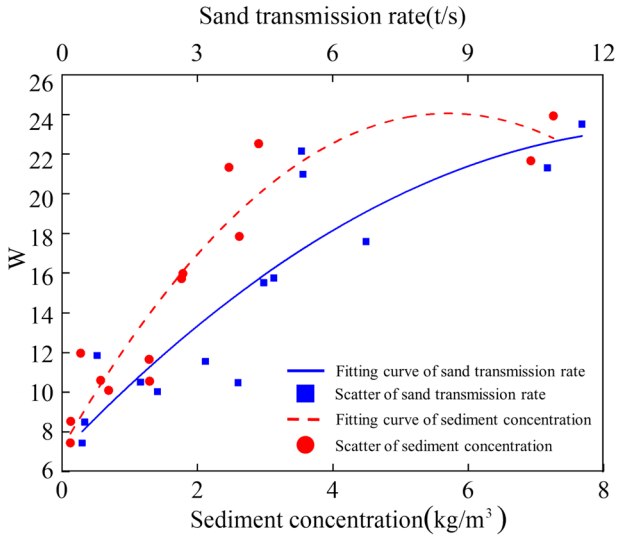

Fig. 8. The correspondence between W and the water and sand conditions.

Discussion

Predictive feasibility analysis

The previous analysis identified the factors influencing the scattering of the water level-discharge relationship and correspondence at HYK hydrographic station and analyzed their interactions through curve fitting. Changes in rating curve are influenced by factors such as water and sand and cross-sectional morphology. The above analysis shows that it is possible and reasonable to predict the water level corresponding to the real-time flow at the HYK section by the rating curve. The data of 2020 is used as an example to verify the feasibility of the method prediction. On the basis of the forecast, the forecast values are compared with the actual data in 2020 to analyze the accuracy of the forecast range.

Analysis of prediction results

(1) Prediction of the fitted curve equation. According to the known information, the pre-flood width-to-depth ratio B of the HYK section to the upstream Tiexie section in 2020 is 309.58. Equations (5) and (6) depicts the fitted curves of B versus the variance S at low and high flow rates.

$$S = -0.0009 \times B^2 + 2.4791 \times B - 1144 \; R^2 = 0.7094 \tag{5}$$

$$S = -0.0024 \times B^2 + 5.8126 \times B - 2276.3 \; R^2 = 0.7728 \tag{6}$$

The predicted variance under low flow in 2020 is − 462.78, and the variance under high flow is − 706.846. The above equation establishes a system of equations to predict the rating curve of HYK in 2018, which is presented as Eq. (7).

$$Z = 0.8264 \ln Q + 83.46 \tag{7}$$

In which, Q represents discharge, and Z represents the water level corresponding to that discharge.

(2) Prediction of the scattered degree of rating curve. Scattering degree can be calculated according to Eq. (8).

$$W = 11786n^2 - 1028.1 * n + 31.285 \tag{8}$$

The roughness of the section of the hydrographic station in HYK before the flood in 2020 is 0.01227. The predicted W value of the HYK section in 2020 is 18.305, which is medium scattering. Plotting the predicted curve against the measured values in the same coordinate system (Fig. 11), it can be found that the predicted results are satisfactory. The difference between the upper and lower envelopes and the predicted result is 0.2%, i.e. the accuracy of the predicted result is within 0.2%. Segmental analysis of different flow levels: when the flow rate is between 1000 and 2800 m^3/s, the prediction curve is located in the center of the point group, and the prediction results are more accurate; when the flow rate is between 2800 and 4000 m^3/s, the prediction results are generally slightly smaller than the measured values. In general, the difference between predicted water level and actual water level is less than 0.4 m[71,72]. It can be regarded that the predicted results are less different from the measured values.

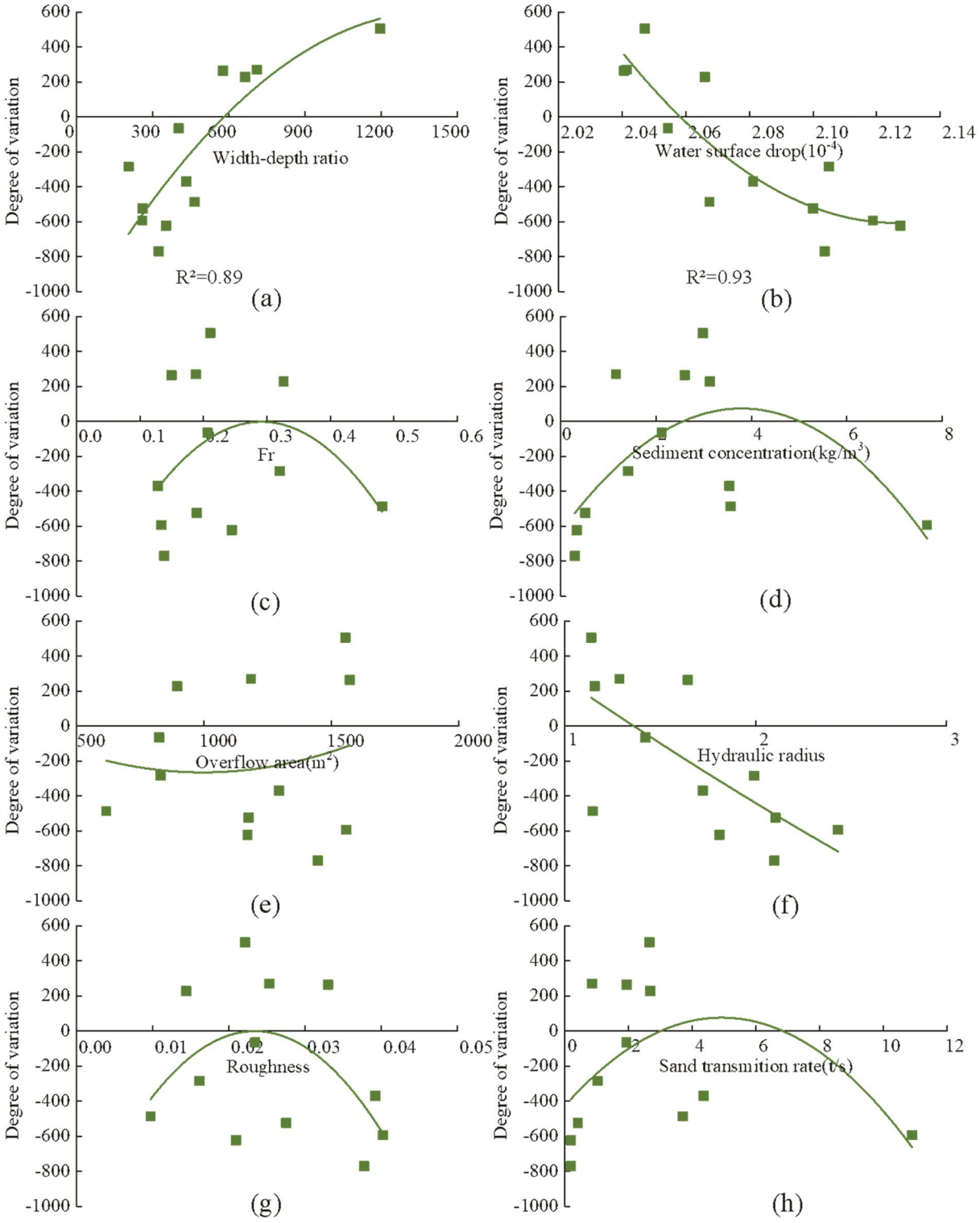

Fig. 9. Factors influencing the degree of variation at low flow rates.

Conclusions

The rating curve was used to predict water level in the lower reaches of the Yellow River. In this study, a complete and reliable water level prediction method based on the rating curve is proposed, taking the HYK hydrological station as an example. The main conclusions of this paper are as follows.

(1) Based on EEMD, the time series of annual mean river discharge and annual mean water level for a total of 72 years, from 1949 to 2020, were decomposed. Mean annual flow in the HYK reach declined significantly before 2000 and stabilized largely after 2000. The mean annual water level was basically stable from the

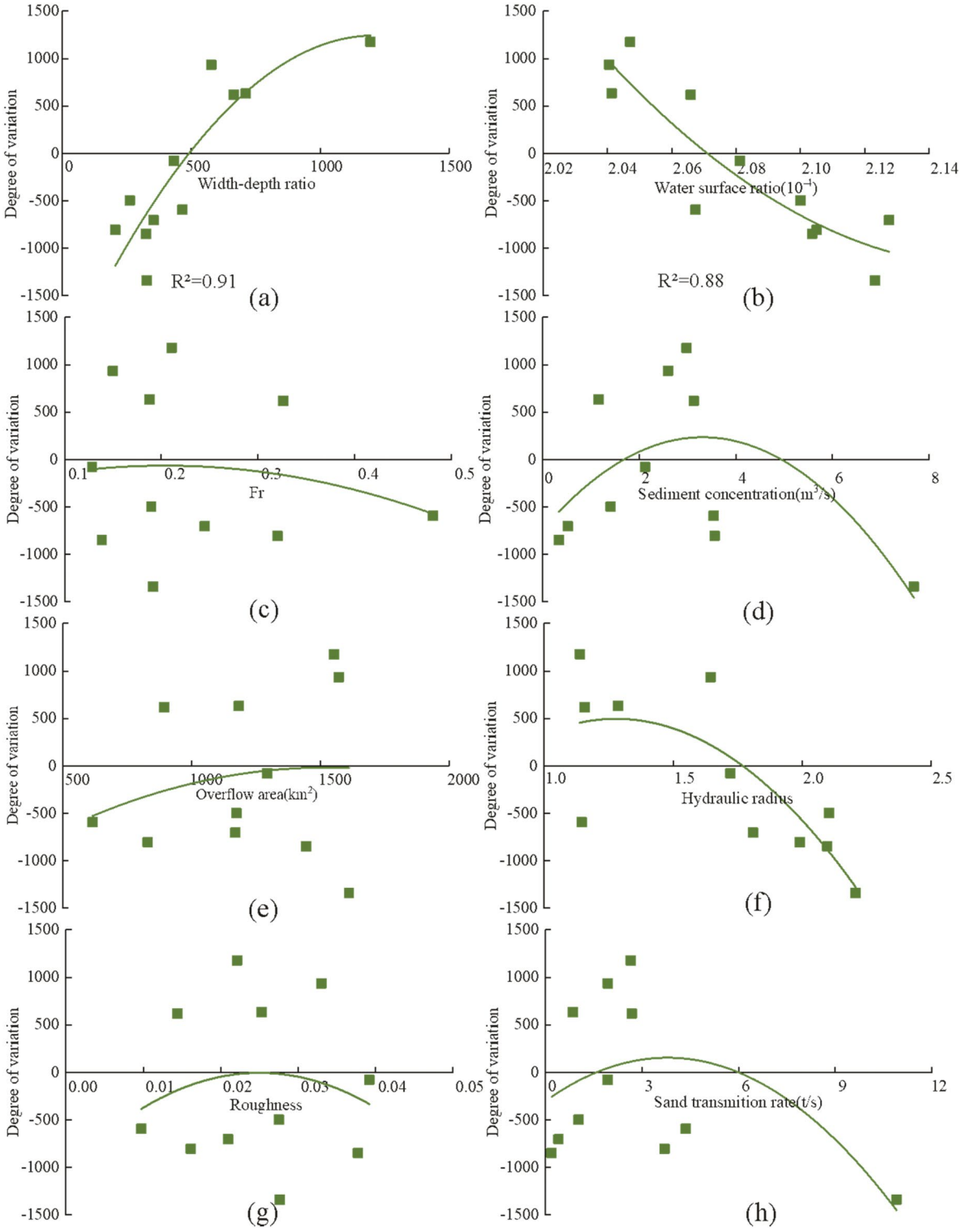

Fig. 10. Factors influencing the degree of variation at high flow rates.

1940s to the 1980s, and after the 1980s, siltation in the lower reaches of the Yellow River improved, and the water level in the HYK declined rapidly.

(2) The construction of the dam resulted in a more stable rating curve at the downstream section. After Sanmenxia Dam, the first dam in the lower reaches of the Yellow River, was put into operation, the daily rating curve at the HYK section changed from a typical rope-jacket type curve to a relatively stable rating curve. After the Long Yangxia Dam and Xiaolangdi Dam were put into operation, the daily average rating curve at the HYK section changed to a more single stable curve in recent years.

(3) The influencing factors of the rating curve were analyzed in terms of both the scattering degree and correspondence of the rating curve. Both section conditions as well as water and sand conditions are important

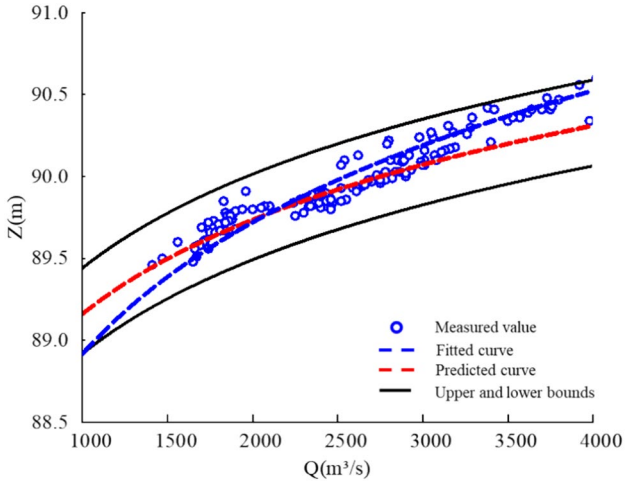

Fig. 11. Comparison of water level prediction results and measured results.

influencing factors for the scattering degree of water level discharge points. The increase of roughness and hydraulic radius will lead to a more stable rating curve. In contrast, the increase of sand content and sand transport rate will lead to a reverse pattern.

(4) This paper verifies the feasibility of the prediction method by using the actual measurement data in 2020 as an example. The predicted 2020 rating curve from the pre-flood section width-to-depth ratio of the HYK is $Z = 0.8264\ln x + 83.46$. The predicted 2020 rating curve using the correlation analysis method is a moderate dispersion, and the predicted 2020 curve and its outer envelope are plotted. The prediction results are relatively consistent with the measured sequence with high accuracy.

Data availability

The data that support the findings of this study are available from Yellow River Institute of Hydraulic Research, YRCC, but restrictions apply to the availability of these data, which were used under license for the current study, and so are not publicly available. Data are however available from the authors upon reasonable request and with permission of Yellow River Institute of Hydraulic Research, YRCC. The datasets analysed during the current study are not publicly available but are available from the corresponding author on reasonable request.

Received: 30 December 2023; Accepted: 28 August 2024
Published online: 07 September 2024

References

1. Quang, N. H. & Viet, T. Q. Long-term analysis of sediment load changes in the Red River system (Vietnam) due to dam-reservoirs. *J. Hydro-Environ. Res.* **51**, 48–66 (2023).
2. Magilligan, F. J. & Nislow, K. H. Changes in hydrologic regime by dams. *Geomorphology* **71**(1–2), 61–78 (2005).
3. Petts, G. E. & Gurnell, A. M. Dams and geomorphology: Research progress and future directions. *Geomorphology* **71**(1–2), 27–47 (2005).
4. Gordon, E. & Meentemeyer, R. K. Effects of dam operation and land use on stream channel morphology and riparian vegetation. *Geomorphology* **82**(3–4), 412–429 (2006).
5. Wyzga, B., Zawiejska, J. & Radecki-Pawlik, A. Impact of channel incision on the hydraulics of flood flows: Examples from Polish Carpathian rivers. *Geomorphology* **272**, 10–20 (2016).
6. Smith, N. D., Morozova, G. S., Perez-Arlucea, M. & Gibling, M. R. Dam-induced and natural channel changes in the below the EB Campbell Dam Canada. *Geomorphology* **269**, 186–202 (2016).
7. Li, S. *et al.* The impacts of the Three Gorges Dam upon dynamic adjustment mode alterations in the Jingjiang reach of the Yangtze River China. *Geomorphology* **318**, 230–239 (2018).
8. Draut, A. E., Logan, J. B. & Mastin, M. C. Channel evolution on the dammed Elwha River, Washington, USA. *Geomorphology* **127**(1–2), 71–87 (2011).
9. Kondolf, G. M., Rubin, Z. K. & Minear, J. T. Dams on the Mekong: Cumulative sediment starvation. *Water Resour. Res.* **50**(6), 5158–5169 (2014).
10. Mei, X. *et al.* Modulation of extreme flood levels by impoundment significantly offset by floodplain loss downstream of the three Gorges Dam. *Geophys. Res. Lett.* **45**(7), 3147–3155 (2018).
11. Liu, W., Wang, S., Sang, Y.-F., Ran, L. & Ma, Y. Effects of large upstream reservoir operations on cross-sectional changes in the channel of the lower Yellow River reach. *Geomorphology* **387**, 107768 (2021).
12. Skalak, K. J. *et al.* Large dams and alluvial rivers in the Anthropocene: The impacts of the Garrison and Oahe Dams on the Upper Missouri River. *Anthropocene* **2**, 51–64 (2013).
13. Lauri, H. *et al.* Future changes in Mekong River hydrology: impact of climate change and reservoir operation on discharge. *Hydrol. Earth Syst. Sci.* **16**(12), 4603–4619 (2012).
14. Fan, J. *et al.* Effects of cascading reservoirs on streamflow and sediment load with machine learning reconstructed time series in the upper Yellow River basin. *Catena* **225**, 107008 (2023).
15. Lehner, B. *et al.* High-resolution mapping of the world's reservoirs and dams for sustainable river-flow management. *Front. Ecol. Environ.* **9**(9), 494–502 (2011).

16. Zarfl, C., Lumsdon, A. E., Berlekamp, J., Tydecks, L. & Tockner, K. A global boom in hydropower dam construction. *Aquat. Sci.* **77**(1), 161–170 (2015).
17. Thieme, M. L. *et al.* Navigating trade-offs between dams and river conservation. *Global Sustain.* **4**, e17 (2021).
18. Yang, W., Yang, H., Yang, D. & Hou, A. Causal effects of dams and land cover changes on flood changes in mainland China. *Hydrol. Earth Syst. Sci.* **25**(5), 2705–2720 (2021).
19. Masaki, Y. *et al.* Intercomparison of global river discharge simulations focusing on dam operation-multiple models analysis in two case-study river basins, Missouri-Mississippi and Green-Colorado. *Environ. Res. Lett.* **12**(5), 055002 (2017).
20. Eldardiry, H. & Hossain, F. The value of long-term streamflow forecasts in adaptive reservoir operation: The case of the high aswan dam in the transboundary Nile River Basin. *J. Hydrometeorol.* **22**(5), 1099–1115 (2021).
21. Ren, S., Zhang, B., Wang, W.-J., Yuan, Y. & Guo, C. Sedimentation and its response to management strategies of the Three Gorges Reservoir, Yangtze River China. *Catena* **199**, 105096 (2021).
22. Wu, Y., Huang, L., Zhao, C., Chen, M. & Ouyang, W. Integrating hydrological, landscape ecological, and economic assessment during hydropower exploitation in the upper Yangtze River. *Sci. Total Environ.* **767**, 145496 (2021).
23. Yang, X. & Lu, X. X. Estimate of cumulative sediment trapping by multiple reservoirs in large river basins: An example of the Yangtze River basin. *Geomorphology* **227**, 49–59 (2014).
24. Bai, T., Wei, J., Chang, F.-J., Yang, W. & Huang, Q. Optimize multi-objective transformation rules of water-sediment regulation for cascade reservoirs in the Upper Yellow River of China. *J. Hydrol.* **577**, 123987 (2019).
25. Jin, W., Chang, J., Wang, Y. & Bai, T. Long-term water-sediment multi-objectives regulation of cascade reservoirs: A case study in the Upper Yellow River China. *J. Hydrol.* **577**, 123978 (2019).
26. Dethier, E. N., Renshaw, C. E. & Magilligan, F. J. Rapid changes to global river suspended sediment flux by humans. *Science* **376**(6600), 1447–1452 (2022).
27. Nilsson, C., Reidy, C. A., Dynesius, M. & Revenga, C. Fragmentation and flow regulation of the world's large river systems. *Science* **308**(5720), 405–408 (2005).
28. Vörösmarty, C. J. *et al.* Anthropogenic sediment retention: Major global impact from registered river impoundments. *Global Planet Change* **39**(1–2), 169–190 (2003).
29. Kong, D., Latrubesse, E. M., Miao, C. & Zhou, R. Morphological response of the Lower Yellow River to the operation of Xiaolangdi Dam China. *Geomorphology* **350**, 106931 (2020).
30. Li, J., Xia, J., Zhou, M., Deng, S. & Zhang, X. Variation in reach-scale thalweg-migration intensity in a braided reach of the lower Yellow River in 1986–2015. *Earth Surf. Process. Landf.* **42**(13), 1952–1962 (2017).
31. Li, J., Xia, J. & Ji, Q. Rapid and long-distance channel incision in the Lower Yellow River owing to upstream damming. *Catena* **196**, 104943 (2021).
32. Burns, A. & Walker, K. F. Effects of water level regulation on algal biofilms in the River Murray South Australia. *Regul. Rivers-Res. Manag.* **16**(5), 433–444 (2000).
33. Chai, Y. *et al.* Evolution characteristics and drivers of the water level at an identical discharge in the Jingjiang reaches of the Yangtze River. *J. Geogr. Sci.* **30**(10), 1633–1648 (2020).
34. Shields, F. D., Simon, A. & Steffen, L. J. Reservoir effects on downstream river channel migration. *Environ. Conserv.* **27**(1), 54–66 (2000).
35. Surian, N., Ziliani, L., Comiti, F., Lenzi, M. A. & Mao, L. Channel adjustments and alteration of sediment fluxes in gravel-bed rivers of north-eastern Italy: Potentials and limitations for channel recovery. *River Res. Appl.* **25**(5), 551–567 (2009).
36. Day, J. W., Cable, J. E., Lane, R. R. & Kemp, G. P. Sediment deposition at the Caernarvon crevasse during the great Mississippi flood of 1927: Implications for coastal restoration. *Water* **8**(2), 385 (2016).
37. Pinter, N. & Heine, R. A. Hydrodynamic and morphodynamic response to river engineering documented by fixed-discharge analysis, Lower Missouri River, USA. *J. Hydrol.* **302**(1–4), 70–91 (2005).
38. Lai, X., Jiang, J., Yang, G. & Lu, X. X. Should the Three Gorges Dam be blamed for the extremely low water levels in the middle-lower Yangtze River?. *Hydrol. Process.* **28**(1), 150–160 (2014).
39. Yang, Y., Zhang, M., Sun, Z., Han, J. & Wang, J. The relationship between water level change and river channel geometry adjustment in the downstream of the Three Gorges Dam. *J. Geogr. Sci.* **28**(12), 1975–1993 (2018).
40. Yang, Y. *et al.* Influence of large reservoir operation on water-levels and flows in reaches below Dam: Case study of the Three Gorges Reservoir. *Sci. Rep.* **7**, 15640 (2017).
41. Han, J., Sun, Z. & Yang, Y. Flood and low stage adjustment in the middle Yangtze River after impoundment of the Three Gorges Reservoir (TGR). *J. Lake Sci.* **29**(5), 1217–1226 (2017) (**in Chinese**).
42. Zhang, M., Zhou, J. & Huang, G. Flood control problems in middle reaches of Yangtze River and countermeasures. *Water Resour. Prot.* **32**(4), 1–10 (2016) (**in Chinese**).
43. Birgand, F., Lellouche, G. & Appelboom, T. W. Measuring flow in non-ideal conditions for short-term projects: Uncertainties associated with the use of stage-discharge rating curves. *J. Hydrol.* **503**, 186–195 (2013).
44. Qiu, J., Liu, B., Yu, X. & Yang, Z. Combining a segmentation procedure and the BaRatin stationary model to estimate nonstationary rating curves and the associated uncertainties. *J. Hydrol.* **597**, 126168 (2021).
45. Haile, A. T., Asfaw, W., Rientjes, T. & Worako, A. W. Deterioration of streamflow monitoring in Omo-Gibe basin in Ethiopia. *Hydrol. Sci. J.* **67**(7), 1040–1053 (2022).
46. Fortesa, J. *et al.* Comparison of stage/discharge rating curves derived from different recording systems: Consequences for stream-flow data and water management in a Mediterranean island. *Sci. Total Environ.* **665**, 968–981 (2019).
47. Haile, A. T., Geremew, Y., Wassie, S., Fekadu, A. G. & Taye, M. T. Filling streamflow data gaps through the construction of rating curves in the Lake Tana sub-basin, Nile basin. *J. Water Climate Change* **14**(4), 1162–1175 (2023).
48. Sahoo, G. B. & Ray, C. Flow forecasting for a Hawaii stream using rating curves and neural networks. *J. Hydrol.* **317**(1), 63–80 (2006).
49. Zhou, X., Revel, M., Modi, P., Shiozawa, T. & Yamazaki, D. Correction of river bathymetry parameters using the stage-discharge rating curve. *Water Resour. Res.* **58**(4), e2021WR031226 (2022).
50. Akhmedova, N. R., Kh Aliyeva, A. & Naumov, V. A. To calculate the maximum annual level according to the water rating curve (on example the small River Zlaya). *IOP Conf. Ser. Earth Environ. Sci.* **1229**(1), 012025. https://doi.org/10.1088/1755-1315/1229/1/012025 (2023).
51. Lee, M. *et al.* Construction of rating curve at high water level considering rainfall effect in a tidal river. *J. Hydrol. Reg. Stud.* **37**, 100907 (2021).
52. Chen, L. *The Evolution of Flow-sediment Series and Channel Responses in the Lower Yellow River after Operation of Xiaolangdi Reservoir* (Master), China Institute of Water Resources & Hydropower Research (IWHR) (2017)
53. Wang, Y., Xia, J., Zhou, M. & Li, J. Characteristics of main channel migration in the braided reach of the Lower Yellow River after the Xiaolangdi Reservoir operation. *Adv. Water Sci.* **30**(2), 198–209 (2019) (**in Chinese**).
54. Bi, N. *et al.* Response of channel scouring and deposition to the regulation of large reservoirs: A case study of the lower reaches of the Yellow River (Huanghe). *J. Hydrol.* **568**, 972–984 (2019).
55. Cheng, Y., Xia, J., Zhou, M. & Wang, Z. Coupled two-dimensional model for heavily sediment-laden floods and channel deformation in a braided reach of the Lower Yellow River. *Appl. Math. Modell.* **131**, 423–437 (2024).

56. Wang, Y. *et al.* Numerical simulation of bank erosion and accretion in a braided reach of the Lower Yellow river. *Catena* **217**, 106456 (2022).
57. Wang, S. & Li, Y. Channel variations of the different channel pattern reaches in the lower Yellow River from 1950 to 1999. *Quat. Int.* **244**, 238–247 (2011).
58. Xia, J., Li, X., Li, T., Zhang, X. & Zong, Q. Response of reach-scale bankfull channel geometry to the altered flow and sediment regime in the lower Yellow River. *Geomorphology* **213**, 255–265 (2014).
59. Hu, H., Tian, G., Wu, Z. & Xia, Q. A study of ecological compensation from the perspective of land use/cover change in the middle and lower Yellow River China. *Ecol. Indic.* **143**, 109382. https://doi.org/10.1016/j.ecolind.2022.109382 (2022).
60. Qu, B., Jiang, E., Li, J., Liu, Y. & Liu, C. Coupling coordination relationship of water resources, eco-environment and socio-economy in the water-receiving area of the Lower Yellow River. *Ecol. Indic.* **160**, 111766. https://doi.org/10.1016/j.ecolind.2024.111766 (2024).
61. Qiao, W. *et al.* Contrasting behaviors of groundwater arsenic and fluoride in the lower reaches of the Yellow River basin, China: Geochemical and modeling evidences. *Sci. Total Environ.* **851**, 158134. https://doi.org/10.1016/j.scitotenv.2022.158134 (2022).
62. Xue, S., Jian, H., Yang, F., Liu, Q. & Yao, Q. Impact of water-sediment regulation on the concentration and transport of dissolved heavy metals in the middle and lower reaches of the Yellow River. *Sci. Total Environ.* **806**, 150535. https://doi.org/10.1016/j.scitotenv.2021.150535 (2022).
63. Zhang, K. *et al.* Allocation of flood drainage rights in the middle and lower reaches of the Yellow River based on deep learning and flood resilience. *J. Hydrol.* **615**, 128560. https://doi.org/10.1016/j.jhydrol.2022.128560 (2022).
64. Lan, H. *et al.* Climate change drives flooding risk increases in the Yellow River Basin. *Geogr. Sustain.* **5**, 193–199. https://doi.org/10.1016/j.geosus.2024.01.004 (2024).
65. Dong, J. *et al.* Effect of water–sediment regulation of the Xiaolangdi Reservoir on the concentrations, bioavailability, and fluxes of PAHs in the middle and lower reaches of the Yellow River. *J. Hydrol.* **527**, 101–112. https://doi.org/10.1016/j.jhydrol.2015.04.052 (2015).
66. Li, W., Zhu, L., Xie, G., Hu, P. & de Vriend, H. J. Quantification of the influencing factors for flood peak discharge increase in the Lower Yellow River. *J. Hydrol.* **613**, 128329. https://doi.org/10.1016/j.jhydrol.2022.128329 (2022).
67. Huang, N. E. *et al.* The empirical mode decomposition and the Hilbert spectrum for nonlinear and non-stationary time series analysis. *Proc. R. Soc. A Math. Phys. Eng. Sci.* **1998**(454), 903–995 (1971).
68. Luo, S. *et al.* Forecasting of monthly precipitation based on ensemble empirical mode decomposition and Bayesian model averaging. *Front. Earth Sci.* **10**, 926067 (2022).
69. Yuan, R. *et al.* Daily runoff forecasting using ensemble empirical mode decomposition and long short-term memory. *Front. Earth Sci.* **9**, 621780 (2021).
70. Ma, B. *et al.* Process-oriented SWMM real-time correction and urban flood dynamic simulation. *J. Hydrol.* **605**, 127269 (2022).
71. Zhao, X. *2D Numerical Modeling for Flow and Sediment Transport in Gaocun-Aishan Reach of the Lower Yelllow River.* (Master), North China Electirc Power University, (2021). (**in Chinese**)
72. Yang, S., Wang, J., Wang, P., Gong, T. & Liu, H. Low altitude unmanned aerial vehicles (UAVs) and satellite remote sensing are used to calculated river discharge attenuation coefficients of ungauged catchments in arid desert. *Water* **11**(12), 2633 (2019).

Author contributions

For this research paper with several authors, a short paragraph specifying their individual contributions was provided. L.M. and Q.L. developed the original idea and contributed to the research design for the study. Z.Z. and Z.L. and H.S. were responsible for data collecting. L.D. and H.C. provided guidance and improving suggestion. N.C., and L.X. provided some guidance for the writing of the article. L.C and S.C provided ideas for the mapping in this paper. All authors have read and approved the final manuscript.

Funding

This work was supported by the National Natural Science Foundation of China, Project No. U2243219 and Outstanding Youth scientific research project of Yellow River Conservancy Commission of the Ministry of Water Resources (HQK-202302).

Competing interests

The authors declare no competing interests.

Additional information

Correspondence and requests for materials should be addressed to C.N. or C.H.